

## Reflection anisotropy and surface electronic structure of W(110)

This article has been downloaded from IOPscience. Please scroll down to see the full text article.

2001 J. Phys.: Condens. Matter 13 L607

(<http://iopscience.iop.org/0953-8984/13/26/104>)

View [the table of contents for this issue](#), or go to the [journal homepage](#) for more

Download details:

IP Address: 171.66.16.226

The article was downloaded on 16/05/2010 at 13:50

Please note that [terms and conditions apply](#).

## LETTER TO THE EDITOR

## Reflection anisotropy and surface electronic structure of W(110)

D S Martin<sup>1,4</sup>, O Zeybek<sup>1</sup>, B Sheridan<sup>1</sup>, S D Barrett<sup>1</sup>, P Weightman<sup>1</sup>,  
J E Inglesfield<sup>2</sup> and S Crampin<sup>3</sup>

<sup>1</sup> Surface Science Research Centre, The University of Liverpool, PO Box 147, Liverpool, L69 3BX, UK

<sup>2</sup> Department of Physics and Astronomy, Cardiff University, PO Box 913, Cardiff, CF24 3YB, UK

<sup>3</sup> Department of Physics, University of Bath, Bath, BA2 7AY, UK

E-mail: davidm@liv.ac.uk

Received 12 April 2001

### Abstract

We report the first measurements of the reflectance anisotropy (RA) spectrum from a body-centred cubic transition metal surface, W(110), and provide a detailed interpretation based upon surface electronic structure calculations. The RA profile exhibits a pronounced resonance feature centred at 3.4 eV which decreases upon oxygen adsorption, indicating a surface effect. Calculating the surface dielectric function within a joint density of states approximation, we identify the important transitions: these are between occupied surface states with a large  $p$ -component to unoccupied  $d$ -states, with the RA arising from the different contributions of  $p_x$  and  $p_y$  states. These surface states have previously been measured using angle-resolved photoemission. The calculated resonance feature occurs at an energy of 2.9 eV, and the difference with experiment is attributed to self-energy effects.

The surface-sensitive optical technique of reflection anisotropy spectroscopy (RAS), originally developed to study semiconductor systems [1], has considerable potential for the study of surfaces in ambient conditions, as demonstrated by recent studies of phase transitions on Au(110) at the solid–liquid interface [2]. However, to fully realise this potential it will be necessary to develop first principles calculations of the surface optical response. Some progress has been made for semiconductor systems where RAS calculations have enabled spectral features to be attributed to surface electronic transitions [3, 4]. The situation is different at metal surfaces, to which RAS is only beginning to be applied. On the (110) surfaces of Cu, Ag, and Au, spectral features have been identified as arising from transitions between surface states [2, 5, 6] and there are indications [7, 8] that some spectral features involve contributions from surface local-field effects [9]. However, there has been no first-principles calculation of the surface optical dielectric response at these metal surfaces, and this has limited progress in interpreting RA spectra.

In this letter we report RAS measurements of W(110), the first on a body-centred cubic transition metal, together with surface electronic structure calculations within a joint densities

<sup>4</sup> Author for correspondence. Fax: +44 151 708 0662.

of states (JDOS) approach which is significantly closer to the surface dielectric response than has been carried out previously for metals. We identify the relevant transitions responsible for the RA of W(110) and show that RAS is probing the same surface states as previously identified using angle-resolved photoemission.

RAS probes as a function of energy the optical response of a surface with linearly polarized light by measuring the difference in normal incidence reflection of two perpendicular directions ( $\Delta r$ ) normalized by the mean reflection ( $r$ ). When RAS is applied to a cubic substrate, surface sensitivity is achieved by the cancellation of contributions involving the electronic structure of the bulk crystal and the RA spectrum arises from the electronic structure of the surface. For W(110) the complex RA is defined in terms of Fresnel reflection amplitudes

$$\frac{\Delta r}{r} = \frac{2(r_{[x]} - r_{[y]})}{r_{[x]} + r_{[y]}} = \frac{2(r_{[001]} - r_{[1\bar{1}0]})}{r_{[001]} + r_{[1\bar{1}0]}} \quad (1)$$

where  $r_{[x]}$  is the complex Fresnel amplitude for reflection of polarized light in the  $x$  crystallographic direction.

Our experiments were performed in an ultra-high vacuum (UHV) environment of base pressure in the  $10^{-11}$  mbar region. A well-ordered, clean W(110) surface was obtained following the standard procedure of oxygen treatment and flashing [10]. The absence of contamination and the presence of surface order was confirmed by x-ray photoelectron spectroscopy and a sharp  $(1 \times 1)$  low-energy electron diffraction (LEED) pattern. The RA spectrometer of the Aspnes design [1] projected and received light through a low-strain window on the UHV system. Experimental artifacts were removed from the spectra using a correction function obtained by measuring spectra with the sample in two orthogonal positions. Real RA spectra were taken over a photon energy range of 1.5 eV to 5.0 eV.

The experimental RA spectrum obtained at room temperature for the clean W(110) surface is shown by curve (a) in figure 1. The RA spectrum is dominated by a strong resonance feature centred at 3.4 eV. In seeking to explain this spectral profile, we note that angle-resolved photoemission experiments on W(110) have shown the existence of an occupied band of surface states over a large fraction of the surface Brillouin zone (SBZ), within  $\sim 1$  eV of the Fermi energy ( $E_F$ ) [11]. An examination of the surface electronic structure of W(110) indicates that candidates for transitions giving rise to the RA spectrum originate from this surface state to unoccupied  $d$ -states at energies above  $E_F$ .

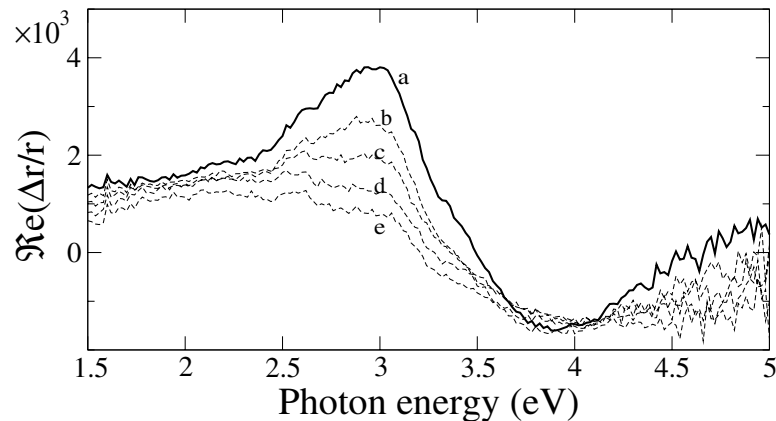


**Figure 1.** (a) Real RA spectra of the clean W(110) surface, and (b)–(e) *in-situ* exposure to oxygen. The sequence of spectra proceed to 0.5 ML coverage.

This interpretation that surface states are involved in the resonance transition is supported by studies of oxygen adsorption. Measurements of the W(110) RA spectra were taken continuously during exposure to O<sub>2</sub> at 300 K, and the results are shown in figures 1(b) to (e). We see that the resonance feature becomes progressively smaller in this sequence of measurements. Studies using the related technique of surface reflection spectroscopy have also shown a change in the optical response of the W(110) surface at  $\sim 3.4$  eV as a function of oxygen exposure [12]. The LEED pattern obtained from the surface corresponding to figure 1(e) indicated coverage of 0.5 ML [13]. The adsorption of O<sub>2</sub> proceeds via dissociation and the O atoms adsorb at the triply coordinated surface sites [14, 15]. The electronic states of atomic O will interact strongly with surface states, and the suppression of the resonance feature on O adsorption is a strong indication that it arises from transitions from surface states. We shall see that this is confirmed by our surface electronic structure calculations.

We calculate the surface electronic structure of W(110) using the scalar relativistic layer-Korringa-Kohn-Rostoker (LKRR) method [16]. In this method, which is based on first calculating the scattering properties within atomic layers and then between layers, an effectively semi-infinite system can be treated. This means that we are dealing with the real surface rather than the surface of a thin slab. This is particularly important for spectral studies where the energy distribution of surface states and bulk states at the surface is required. The atomic sphere approximation is used to describe the potential, extended into the vacuum: we calculate a spherically symmetric potential within each atomic sphere self-consistently, within the local density approximation (LDA). The atomic sphere approximation is known to work well for the fairly close-packed body-centred cubic (110) surface.

For interpreting the RA spectrum, we calculate the surface joint density of states (JDOS) [17], decomposed into angular momentum components [12]. As the surface wavevector  $\mathbf{K}$  of the initial and final states is the same in the optical transition, this JDOS is defined as

$$Z_{L,L'}(E) = \sum_{i,f} \delta(E - E_f + E_i) \delta(\mathbf{K}_i - \mathbf{K}_f) \int d\mathbf{r} |\psi_{i,L}(\mathbf{r})|^2 \int d\mathbf{r}' |\psi_{f,L'}(\mathbf{r}')|^2. \quad (2)$$

The summations extend over all occupied initial states  $i$  and unoccupied final states  $f$ . The integrals are over the surface atomic sphere, and  $\psi_{i,L}$ ,  $\psi_{f,L'}$  are the components of the initial and final state wavefunctions with angular momentum  $L$  and  $L'$ . There is excellent convergence with respect to the wavevector summation, and we sum over 256  $\mathbf{K}$  points in the irreducible part of the surface Brillouin zone, with an energy broadening of 0.05 eV. The imaginary part of the surface dielectric function for  $y$  polarization can then be found, approximately, in terms of the JDOS components

$$\epsilon''_y \propto \sum_{L,L'} Z_{L,L'} |\langle L|y|L' \rangle|^2 \quad (3)$$

with a similar expression for the  $x$  polarization. The optical matrix element imposes the dipole selection rules on  $L$  and  $L'$ , and it is the difference in surface dielectric function with the two polarizations which gives rise to the RA.

Analysis of the JDOS shows that the main contribution to the surface dielectric function is in  $y$ -polarization, that is, with the electric field in the  $[1\bar{1}0]$  direction. This comes from transitions between occupied surface states with a large  $p_y$  component, rather than  $d_{yz}$  as originally proposed [11, 18], and unoccupied  $d_{3z^2-r^2}$  states. The surface states make a much smaller contribution to  $\epsilon_x$ , corresponding to polarization in the  $[001]$  direction, because they have a much smaller  $p_x$  component overall. The upper panel of figure 2 shows  $\Delta Z_{y/x \rightarrow 3z^2-r^2}$ , defined as

$$\Delta Z_{y/x \rightarrow 3z^2-r^2} = Z_{y,3z^2-r^2} - Z_{x,3z^2-r^2}. \quad (4)$$

The double peak between 1 eV and 3 eV comes from surface states with a large  $p_y$  component in the lighter shaded region of the surface Brillouin zone shown in figure 3, just below the Fermi

energy. The minimum between the peaks at 2.4 eV comes from transitions between surface states with a large  $p_x$  component and unoccupied  $d_{3z^2-r^2}$  cancelling out the  $p_y \rightarrow d_{3z^2-r^2}$  transitions. These  $p_x$  states occur in the darker shaded region of the surface Brillouin zone (figure 3). Just as  $Z$  corresponds to the imaginary part of the dielectric function, so its Hilbert transform  $\hat{Z}$  corresponds to the real part of  $\epsilon$ . The dashed line in figure 2 shows the Hilbert transform of the difference in JDOS,  $\Delta\hat{Z}$ , and we see that the combination of peaks and the minimum in  $\Delta Z$  gives rise to a resonance structure at 2.9 eV, of the shape seen in RAS.

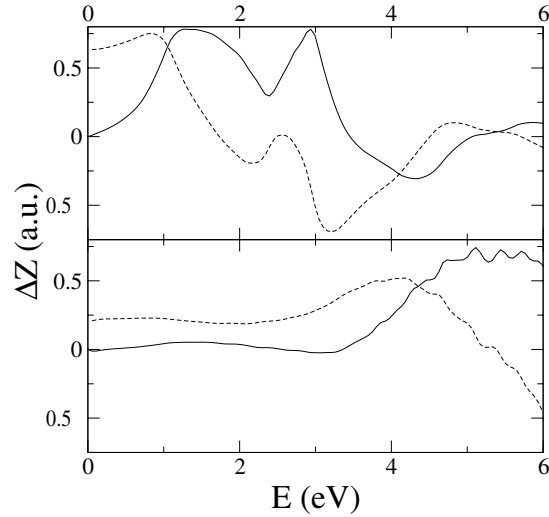


**Figure 2.** Difference in joint densities of states at W(110) between the transitions  $p_y \rightarrow d_{3z^2-r^2}$  and  $p_x \rightarrow d_{3z^2-r^2}$  (upper panel), and  $d_{x^2-y^2} \rightarrow p_y$  and  $d_{x^2-y^2} \rightarrow p_x$  (lower panel). The solid curves show  $\Delta Z$  (the JDOS difference), and the dashed curves  $\Delta\hat{Z}$  (its Hilbert transform).

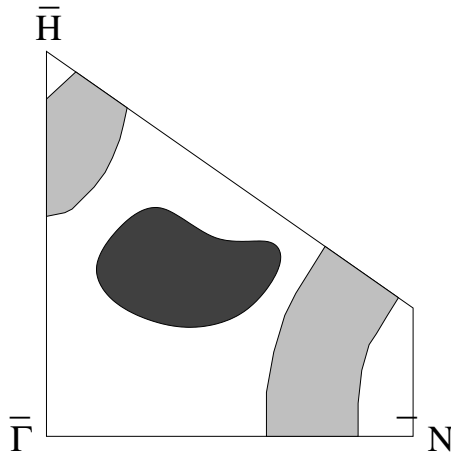


**Figure 3.** Irreducible part of the W(110) surface Brillouin zone. Light shading indicates the region where the main  $p_y \rightarrow d_{3z^2-r^2}$  transitions occur, and heavy shading indicates where there are transitions from  $p_x \rightarrow d_{3z^2-r^2}$ , with an energy of about 2.5 eV.

The only other dipole-active transitions which contribute significantly to RAS are between occupied states with  $d_{x^2-y^2}$  character and unoccupied states with an appreciable  $p_y$  component. These transitions have a higher energy, around 5 eV, and the corresponding  $\Delta Z_{x^2-y^2 \rightarrow y/x}$  is shown in the lower half of figure 2, together with its Hilbert transform. The states in these transitions cannot easily be identified with particular surface states as in the lower-energy transitions. One point which should be emphasized is that these are all surface effects. By the second layer of atoms, the  $p_x$  and  $p_y$  contributions to the densities of states are very close.

To proceed further it is necessary to estimate  $\Delta r/r$ . A full calculation of this is beyond current capabilities, so instead we use an overlayer model based on Fresnel theory [19, 20]. We treat the surface as a thin overlayer with a surface dielectric anisotropy  $\Delta\tilde{\epsilon}_s = \tilde{\epsilon}_x - \tilde{\epsilon}_y$ , on top of the bulk with an isotropic dielectric function  $\tilde{\epsilon}_b$ . The reflectance amplitudes are related to the surface and bulk dielectric functions by

$$\frac{\Delta r}{r} = \frac{2i\omega d}{c} \left( \frac{\Delta\tilde{\epsilon}_s}{\tilde{\epsilon}_b - 1} \right) \quad (5)$$

where  $d$  is the surface layer thickness and  $\omega$  is the frequency. This result is valid for small anisotropy and within the thin film approximation, assuming also the validity of Fresnel optics in this context. Bulk dielectric function data for tungsten were obtained from experimentally tabulated data [21] and used to determine the functions  $A(\omega)$  and  $B(\omega)$  defined by

$$A(\omega) - iB(\omega) = \frac{1}{1 - \tilde{\epsilon}_b(\omega)}. \quad (6)$$

The contribution to  $\Re(\Delta r/r)$  from the JDOS between the occupied  $p_y, p_x$  and unoccupied  $d_{3z^2-r^2}$  states is then

$$\Re\left(\frac{\Delta r}{r}\right) \propto \omega[A(\omega)\Delta Z_{y/x \rightarrow 3z^2-r^2} + B(\omega)\Delta\tilde{Z}_{y/x \rightarrow 3z^2-r^2}] \quad (7)$$

with a similar expression for the contribution from the other dipole-active transitions.

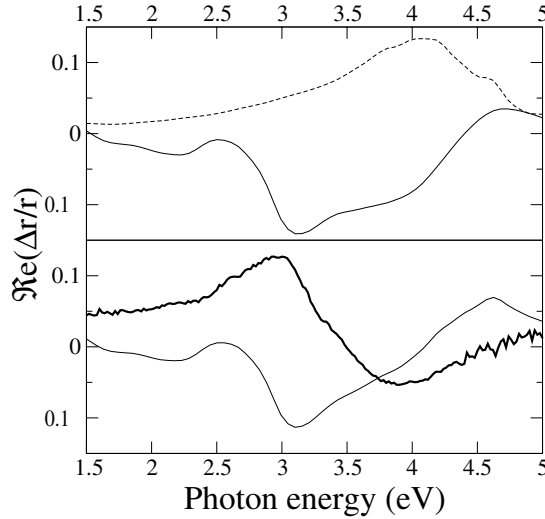


**Figure 4.** Upper panel: contributions to  $\Delta r/r$  from the transitions  $p_{y/x} \rightarrow d_{3z^2-r^2}$  (solid line) and  $d_{x^2-y^2} \rightarrow p_{y/x}$  (dashed line). These results are without matrix elements and the prefactor in equation (7). Lower panel: calculated (thin line) and experimental (thick line) RA profile. The experimental curve has been scaled to match the absolute magnitude of the theoretical curve.

The contributions to the reflection anisotropy from the significant dipole-active transitions are shown in the upper panel of figure 4. We see that the resonance feature at 2.9 eV from the  $p_{y/x} \rightarrow d_{3z^2-r^2}$  transitions persists, whereas the higher energy  $d_{x^2-y^2} \rightarrow p_{y/x}$  transitions give a positive background at lower photon frequencies and a broad feature at about 4 eV. Since we are unable at this stage to calculate the absolute values of the matrix elements in equation (3) it is not possible to calculate the absolute magnitude of the RA or the relative intensity of the two contributions to it. However, we find the shape of the RA spectrum from these

results by treating the relative intensity as a free parameter. The result obtained by combining  $p_{y/x} \rightarrow d_{3z^2-r^2}$  with half of  $d_{x^2-y^2} \rightarrow p_{y/x}$  is compared with the experimental data in the lower panel of figure 4. The experimental  $\Re(\Delta r/r)$  values have been scaled by a constant multiplicative factor to match the absolute magnitude of the theoretical curve. We see that our theoretical approach obtains structure which is comparable with experiment.

The comparison between theory and experiment in the lower panel of figure 4 shows that the calculated resonance has too low an energy, by about 0.5 eV. This is probably due to many-body effects—the neglect of the energy-dependent self-energy in our calculation. There are indications in the RAS data of a peak at about 5 eV and this is also consistent with our results of figure 4 shifted to higher energies. Now the bulk W density of states shows a pronounced dip between the occupied and unoccupied states, and we would expect that many-body corrections to the LDA band structure as calculated in the GW approximation [22] would have similar behaviour to the self-energy in a semiconductor—increasing the separation between states, hence increasing the energy of the RA spectral features. To the best of our knowledge, there have been no calculations of the W self-energy to date, but an increase in energy of unoccupied states relative to band calculations is found in inverse photoemission studies on W(110) [23].

To conclude, we have presented the first RAS results for a bcc material, W(110), and the first JDOS interpretation of the spectrum from metals. Our experimental results together with the identification of the surface states involved in the transitions shows that RAS combined with first-principles calculations has great potential as a probe of metal surface electronic structure. Here we are probing the same surface states as in angle-resolved photoemission but RAS has the advantage that it can be used as an *in-situ* probe of surfaces in different environments. This study shows that a simple treatment of surface optical response can work well, whilst highlighting that advanced calculations of the surface dielectric function will be particularly useful in the future.

The authors acknowledge the UK EPSRC for support of this work.

## References

- [1] Aspnes D 1988 *Appl. Phys. Lett.* **52** 957
- [2] Sheridan B *et al* 2000 *Phys. Rev. Lett.* **85** 4618
- [3] Sobiesierski Z, Westwood D I and Matthai C C 1998 *J. Phys.: Condens. Matter* **10** 1
- [4] Manghi F *et al* 1990 *Phys. Rev. B* **41** 9935
- [5] Hofmann Ph *et al* 1995 *Phys. Rev. Lett.* **75** 2039
- [6] Stahrenberg K *et al* 1998 *Phys. Rev. B* **58** R10207
- [7] Hansen J-K, Bremer J and Hunderi O 1998 *Phys. Status Solid a* **170** 271
- [8] Borensztein Y *et al* 1993 *Phys. Rev. Lett.* **71** 2334
- [9] Mochán W L and Barrera R G 1986 *Phys. Rev. Lett.* **56** 2221
- [10] Becker J A, Becker E J and Brandes R G 1961 *J. Appl. Phys.* **32** 411
- [11] Holmes M W, King D A and Inglesfield J E 1979 *Phys. Rev. Lett.* **42** 394
- [12] Blanchet G B and Stiles P J 1980 *Phys. Rev. B* **21** 3273
- [13] Germer L H and May J W 1966 *Surf. Sci.* **4** 452
- [14] Van M A Hove and Tong S Y 1975 *Phys. Rev. Lett.* **35** 1092
- [15] Johnson K E, Wilson R J and Chiang S 1993 *Phys. Rev. Lett.* **71** 1055
- [16] Maclaren J M *et al* 1990 *Comput. Phys. Commun.* **60** 365
- [17] Ibach H and Lüth H 1993 *Solid-State Physics* (Berlin: Springer)
- [18] Blanchet G B, Estrup P J and Stiles P J 1981 *Phys. Rev. B* **23** 3655
- [19] Cole R J, Frederick B G and Weightman P 1998 *J. Vac. Sci. Technol. A* **16** 3088
- [20] McIntyre J D E and Aspnes D E 1971 *Surf. Sci.* **24** 417
- [21] Lynch D W and Hunter W R 1985 *Handbook of Optical Constants of Solids* ed E Palik (New York: Academic)
- [22] Godby R W 1992 *Unoccupied Electronic States* ed J C Fuggle and J E Inglesfield (Berlin: Springer)
- [23] Li D *et al* 1993 *Phys. Rev. B* **47** 12 895